

# High-Performance Biodegradable Films from Bamboo Derived Cellulose Nanofibers and Silk Fibroin: Engineering Sustainable Polymer Composites

J.Lurdhumary<sup>1</sup>, K. Alagarraja<sup>2</sup>, S.karthikeyan<sup>3</sup>, Sathyaseelan. P<sup>4</sup>, P. Sobhanachalam<sup>5</sup>, P. Nantha kumar<sup>6</sup>, Kirubakaran D<sup>7</sup>, Nellore Manoj Kumar<sup>8</sup>, Sudhakar M<sup>9,\*</sup>

## Abstract

*This research presents the advancement of biodegradable composite films from cellulose nanofibers (CNFs) extracted from bamboo and silk fibroin (SF) derived from Bombyx mori cocoons. CNF/SF composites were fabricated in three different compositions—CS10, CS30, and CS50—via aqueous blending and solution casting, followed by ethanol-induced  $\beta$ -sheet stabilization. Mechanical testing confirmed a considerable enhancement in tensile strength from 72 MPa (CS10) to 112 MPa (CS50), while Young's modulus improved from 2.4 GPa to 4.8 GPa, and elongation at break improved from*

*3.1% to 6.8%, demonstrating a synergistic balance between stiffness and ductility. Thermogravimetric analysis indicated a rise in onset degradation temperature from 262 °C (CS10) to 298 °C (CS50), confirming improved thermal resilience due to  $\beta$ -sheet crystallization and hydrogen bonding. Surface wettability analysis showed an increase in water contact angle from 64° to 74° with increasing SF content, implying enhanced hydrophobicity. Water absorption decreased from 45% to 28%, correlating with reduced hydroxyl accessibility. FTIR analysis confirmed molecular interactions through intensified Amide I (~1650  $\text{cm}^{-1}$ ) and Amide II (~1515  $\text{cm}^{-1}$ ) peaks and diminished O–H stretching (~3300  $\text{cm}^{-1}$ ), supporting hydrogen bonding between CNFs and SF. The CS50 composite displayed optimal performance, suggesting its suitability for flexible, moisture-resistant biodegradable applications in biomedical and packaging sectors, providing a green alternative to petroleum-derived plastics.*

### \*Author for Correspondence

Sudhakar M  
E-mail: sudhakar3686@gmail.com

<sup>1</sup>Assistant Professor, Department of Electronics and Communication Engineering, Sri Sairam Institute of Technology, Chennai, Tamil Nadu, India

<sup>2</sup>Assistant Professor, Department of Mechanical Engineering, New Prince Shri Bhavani College of Engineering and Technology, Chennai, Tamil Nadu, India

<sup>3</sup>Professor, Department of Electronics and Communication Engineering, Sathyabama institute of science and technology, Chennai, Tamil Nadu, India

<sup>4</sup>Associate Professor, Department of Mechanical, Vel Tech Rangarajan Dr.Sangunthala R&D Institute of science and Technology, Chennai, Tamil Nadu, India

<sup>5</sup>Associate Professor, Department of Physics (FED), Lakireddy Bali Reddy College of Engineering, Mylavaram, Andhra Pradesh, India

<sup>6</sup>Associate Professor, Department of Mechanical Engineering, Sri Sairam Engineering College, Chennai, Tamil Nadu, India

<sup>7</sup>Professor, Department of Electrical and Electronics Engineering, St. Joseph's Institute of Technology, Chennai, Tamil Nadu, India

<sup>8</sup>Adjunct Faculty, Department of Mathematics, Saveetha School of Engineering, Saveetha Institute of Medical and Technical Sciences (SIMATS), Thandalam, Chennai, Tamil Nadu, India

<sup>9</sup>Assistant Professor, Department of Mechanical Engineering, Sri Sairam Engineering College, Sai Leo Nagar, West Tambaram, Chennai, Tamil Nadu, India

Received Date: June 06, 2025

Accepted Date: June 23, 2025

Published Date: July 17, 2025

**Citation:** J.Lurdhumary, K. Alagarraja, S.karthikeyan, Sathyaseelan. P, P. Sobhanachalam, P. Nantha kumar, Kirubakaran D, Nellore Manoj Kumar, Sudhakar M. High-Performance Biodegradable Films from Bamboo Derived Cellulose Nanofibers and Silk Fibroin: Engineering Sustainable Polymer Composites. Journal of Polymer & Composites. 2025; 13(4): 256–265p.

**Keywords:** Cellulose nanofibers (CNFs), silk fibroin (SF), biodegradable composites, hydrogen bonding, thermal and mechanical properties

## INTRODUCTION

In recent years, the global demand for sustainable materials has intensified because of growing ecological issues such as poor biodegradability, dependence on fossil fuels, and ecological toxicity [1,2]. The accumulation of non-degradable plastic waste has become a critical issue, prompting researchers and industries to explore eco-friendly

alternatives that meet the functional requirements of structural and consumer products [3,4]. Among the various natural biopolymers, cellulose and silk fibroin have emerged as promising candidates for developing high-performance biodegradable materials [5–7].

Cellulose, the most common natural polymer on earth, is derived primarily from plant biomass [8]. Its nanoform, known as cellulose nanofibers (CNFs), offers a unique combination of high strength, and crystallinity [9,10]. These nanofibers also possess a high specific surface area and excellent reinforcing ability when dispersed in polymer matrices, making them ideal for green composite development [11]. Bamboo is one of the most renewable and rapidly growing sources of cellulose and has gained popularity due to its low cost, fast harvest cycle, and high fiber yield [12,13]. Bamboo-derived CNFs have shown improved reinforcement capabilities compared to conventional wood pulp due to their finer microstructure and higher cellulose content [14].

Conversely, silk fibroin (SF), derived from the cocoons of *Bombyx mori*, is a biopolymer well recognized for its excellent mechanical strength, biodegradability, and compatibility with biological systems [15]. Fibroin consists of repetitive amino acids that facilitate the formation of  $\beta$ -sheet crystallites, conferring tensile strength and stability to silk-based films and fibers [16,17]. In addition to its structural characteristics, SF is also being investigated for its non-toxic degradation behaviour [18,19].

Combining CNFs and SF into a single composite structure allows for synergistic interaction, where the cellulose phase offers mechanical rigidity and load-bearing capacity, while the silk matrix contributes ductility, biodegradability, and interfacial adhesion [20]. Such hybrid composites are expected to overcome limitations associated with each component when used independently. For instance, while CNFs may suffer from brittleness or moisture sensitivity, the presence of silk fibroin can introduce flexibility and improved water resistance, making the resulting material suitable for biodegradable packaging, medical textiles, and green electronics [21,22].

Furthermore, CNFs and SF are both processable via aqueous-phase casting and are compatible with low-temperature fabrication routes, ensuring energy-efficient and scalable manufacturing [23]. Non-covalent interactions significantly improve interfacial adhesion, eliminating the requirement for chemical cross-linkers [24,25]. Additionally, these composites hold potential for functional modifications including UV shielding, antioxidant incorporation, and antimicrobial behaviour through surface treatment or additive blending [26,27].

As the demand for green composites accelerates in fields like biomedicine, food packaging, and structural materials, the present study investigates the fabrication, characterization, and performance of bamboo-derived cellulose nanofiber/silk fibroin composites. Unlike petroleum-derived plastics, these biocomposites offer a closed-loop lifecycle with minimal ecological footprint, positioning them as strategic alternatives for future material ecosystems [28–30].

## MATERIALS AND METHODS

### Materials

Mature stems of *Bambusa vulgaris* were utilized to obtain bamboo powder, which was acquired from a regional processing facility in Kerala, India. Silk cocoons from *Bombyx mori* were sourced through the Central Silk Board of India. All chemicals employed in the experiments—including sodium hydroxide (NaOH), lithium bromide (LiBr), sodium chlorite (NaClO<sub>2</sub>), glacial acetic acid, ethanol, and distilled water—were of analytical grade.

### Extraction of Cellulose Nanofibers (CNFs) from Bamboo

*Step 1: Alkali treatment (delignification):* Bamboo powder was oven-dried (Figure 1) and treated with 5% (w/v) NaOH solution in a solid-to-liquid ratio of 1:20 (w/v) at 80°C for 3 hours under continuous stirring to remove lignin and hemicellulose.

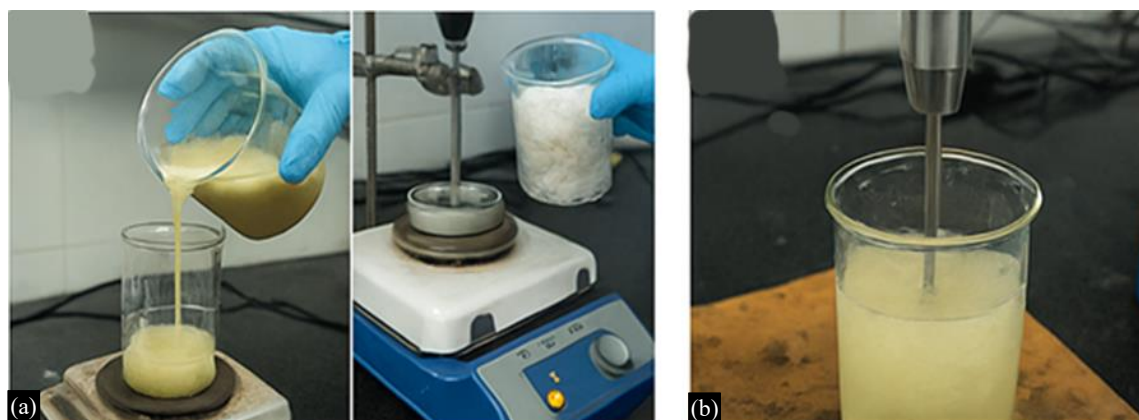


**Figure 1.** Extraction of cellulose nanofibers (CNFs) from bamboo. (a) Alkali Treatment (Delignification) & Bleaching, (b) Mechanical Fibrillation.

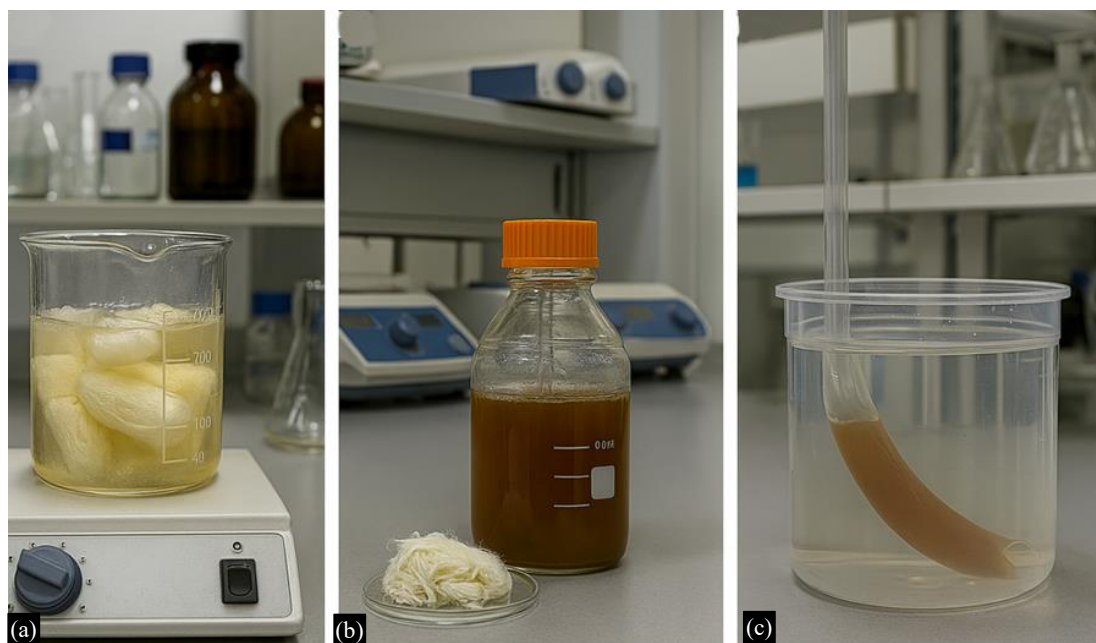


**Figure 2.** Preparation of silk fibroin (SF) solution. (a) Degumming, (b) Dissolution (c) Dialysis

*Step 2: Bleaching:* The alkali-treated fibers were bleached with an acidified sodium chlorite solution (1.7%  $\text{NaClO}_2$  and 0.6 mL acetic acid per 100 mL) at  $70^\circ\text{C}$  for 2 hours. This step was repeated twice to obtain a white cellulose pulp. The product was again washed to neutrality and stored wet.

*Step 3: Mechanical fibrillation:* The bleached cellulose pulp was dispersed in water (1 wt%) and subjected to high-shear homogenization using a high-pressure homogenizer (20,000 rpm) for 5 cycles to produce cellulose nanofibers. The solution was stored at  $5^\circ\text{C}$  for subsequent blending.

### Preparation of Silk Fibroin (SF) Solution

*Step 1: Degumming:* To eliminate sericin, Bombyx mori cocoons were treated by boiling in a 0.03 M sodium carbonate ( $\text{Na}_2\text{CO}_3$ ) solution for 30 minutes (Figure 2). The resulting degummed fibroin fibers were then left to dry.

*Step 2: Dissolution:* Dried silk fibroin was dissolved in an aqueous lithium bromide (LiBr) solution with a concentration of 9.4 M at  $65^\circ\text{C}$  for 5 hours, maintaining a weight-to-volume ratio of 1:4 between the silk and the solvent.

*Step 3: Dialysis:* To eliminate lithium bromide, the silk/LiBr mixture was subjected to dialysis using distilled water as the dialysate. The water was replaced every 6 hours over a period of 72 hours. The final fibroin concentration was estimated gravimetrically and adjusted to ~6 wt%.

### **Preparation of CNF/SF Composite Films**

#### ***Blending and casting***

The CNF suspension and SF solution were mixed in various ratios by weight:

CS10: 90% CNF / 10% SF

CS30: 70% CNF / 30% SF

CS50: 50% CNF / 50% SF

The mixtures were magnetically stirred for 2 hours to ensure homogeneity. Air bubbles were removed via sonication (ultrasonic bath, 40 kHz, 15 minutes). The mixture was poured into Teflon-coated petri dishes and allowed to dry under room temperature conditions for 48 hours, resulting in uniform biocomposite films with an approximate thickness of 0.2 mm.

#### **Post-Treatment for Structural Stabilization**

To promote  $\beta$ -sheet structure development and render the silk fibroin component water-insoluble, the dried films were soaked in 90% ethanol for one hour, followed by air drying.

### **Techniques for Material Characterization**

#### ***Mechanical testing***

Mechanical properties were evaluated using a universal testing machine (Instron 3365). Samples were prepared as rectangular strips measuring 50 mm  $\times$  10 mm and tested as per the ASTM D882 standard. Each result was averaged over five replicates.

#### ***Thermal stability (TGA)***

Thermal and decomposition characteristics were studied using TGA, (PerkinElmer) from 35°C to 650°C at a heating rate of 15°C/min. Weight loss curves were used to evaluate onset decomposition temperature and residual mass.

#### ***Water contact angle (WCA)***

A contact angle goniometer (Krüss GmbH) was used in this study. A 5  $\mu$ L drop of distilled water was gently dispensed onto the film surface, and the contact angle was noted within 10 seconds. Measurements were taken at five distinct points on each sample to ensure accuracy.

#### ***Water absorption test***

Dried film samples with known initial weights were submerged in distilled water at ambient temperature for 24 hours. After soaking, excess surface water was gently removed, and the samples were weighed again. Water absorption (%) was calculated as:

$$WA\% = [(W_{\text{wet}} - W_{\text{dry}}) / W_{\text{dry}}] \times 100$$

#### ***Fourier transform infrared spectroscopy (FTIR)***

FTIR spectra of individual components (CNF, SF) and composite films were recorded in the range 4000–500  $\text{cm}^{-1}$  using an ATR-FTIR spectrometer (Bruker Alpha). Spectra were used to verify intermolecular interactions and structural transitions (e.g.,  $\beta$ -sheet formation).

## **RESULTS AND DISCUSSION**

### **Mechanical Properties**

The tensile behaviour of the CNF/SF composite films was assessed, with the corresponding results illustrated in Figure 3 and detailed in Table 1.

**Table 1.** Mechanical, Thermal, and Surface Properties of CNF/SF Composites.

Composite	Tensile strength (MPa)	Young's modulus (GPa)	Elongation at break (%)	Onset degradation temp (°C)	Water contact angle (°)
CS10	72	2.4	3.1	262	64
CS30	98	3.7	4.5	282	68
CS50	112	4.8	6.8	298	74

The CS10 formulation, consisting of 90% cellulose nanofibers (CNFs) and 10% silk fibroin (SF), showed enhanced mechanical behavior, with tensile strength reaching 72 MPa and stiffness (Young's modulus) recorded at 2.4 GPa. CS30, with a higher SF ratio (30%), demonstrated significantly improved strength, reaching 98 MPa with a modulus of 3.7 GPa. CS50, which had an equal weight ratio of CNF and SF, achieved the highest property values.

This trend is attributed to synergistic mechanical reinforcement between the two biopolymers. Specifically, the hydroxyl groups on CNFs readily form hydrogen bonds, leading to efficient stress transfer across the CNF–SF interface [21,22].

Moreover, silk fibroin undergoes a conformational transformation into  $\beta$ -sheet structures during ethanol post-treatment, which act as physical cross-links, enhancing the matrix stiffness and contributing to the observed increase in modulus [23]. The  $\beta$ -sheet domains function as load-bearing crystalline regions that arrest polymer chain slippage, resulting in higher resistance to deformation under tensile load.

The elongation at break also improved markedly from 3.1% for CS10 to 6.8% for CS50. This is somewhat counterintuitive, as increased crystallinity typically reduces elongation. However, in this case, the flexible protein backbone of SF imparts ductility, and the entangled structure between CNFs and SF provides energy dissipation pathways, enabling composites to sustain higher deformation before failure [24].

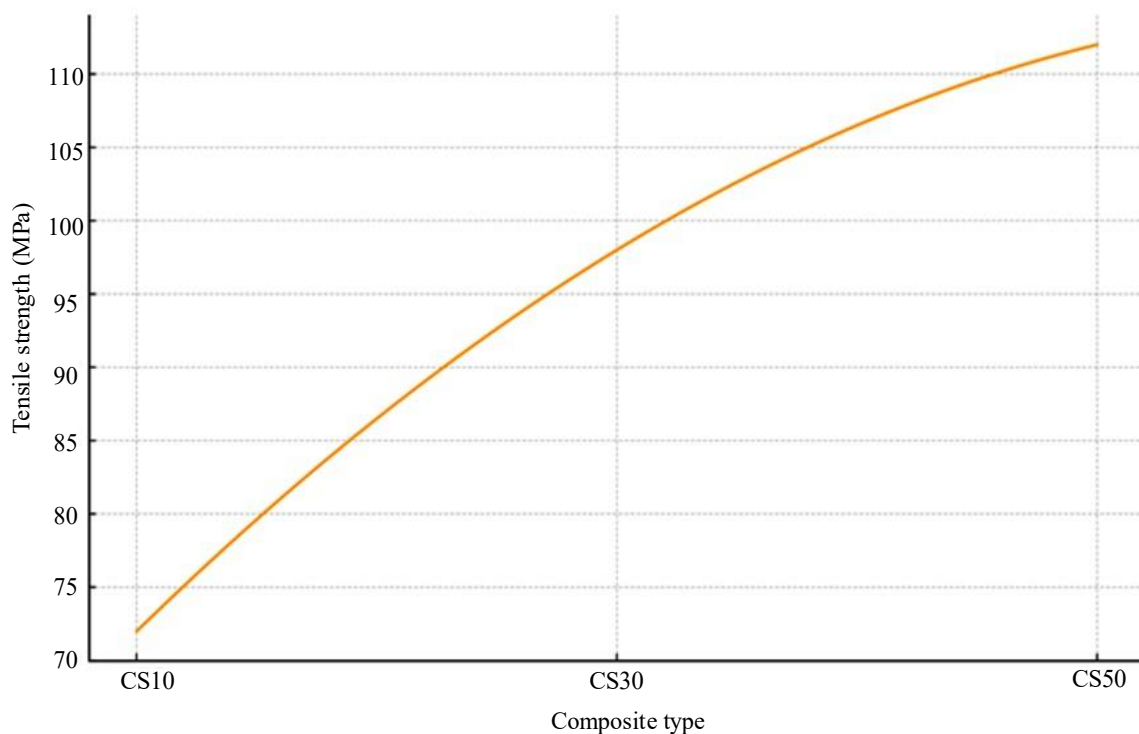


**Figure 3.** Tensile strength of CNF/SF composites.

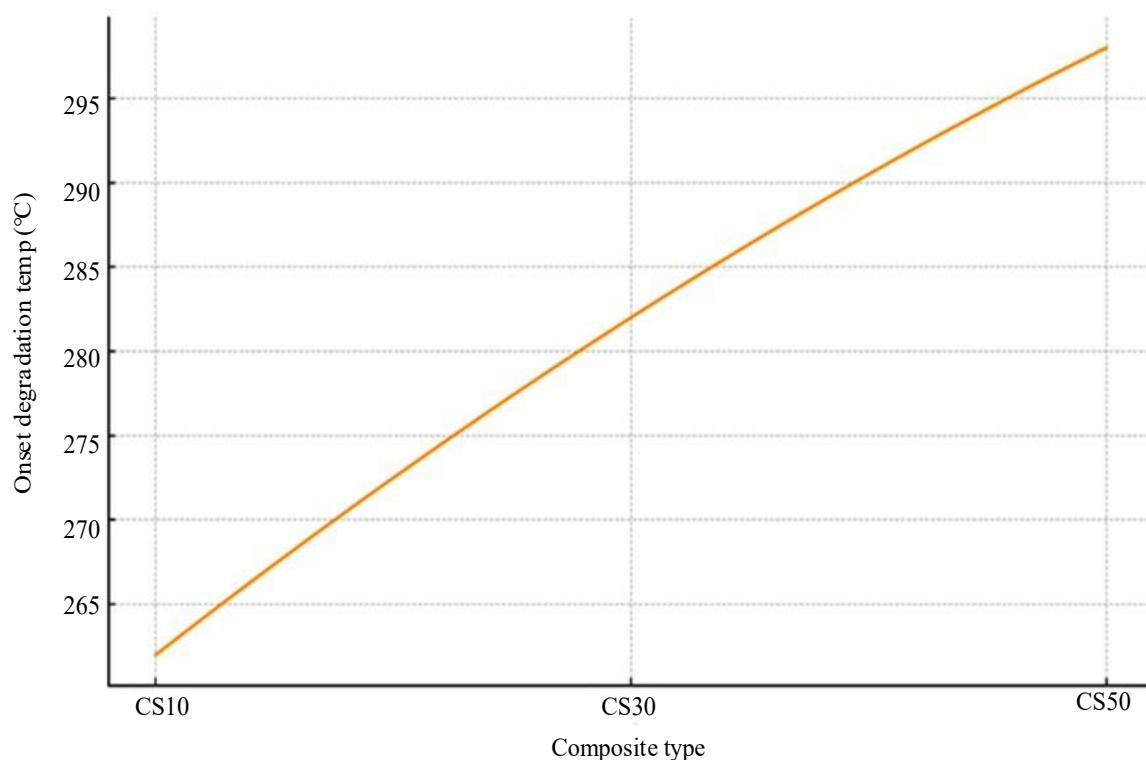


**Figure 4.** Thermal Stability (TGA Onset Temp).

Such combined improvements in stiffness, strength, and ductility position the CNF/SF composites; especially CS50—as a compelling choice for applications requiring biodegradable and flexible films, such as biomedical dressings, packaging, and flexible electronics [25].

#### Thermal Stability (TGA Analysis)

The onset degradation temperature ( $T_{\text{onset}}$ ), which denotes the point of major polymer chain scission, was observed to improve significantly with increasing SF content (Figure 4).

CS10 began decomposing at 262°C, characteristic of typical CNF-rich systems.

CS30 exhibited improved  $T_{\text{onset}}$  at 282°C, indicating enhanced thermal resilience.

CS50 showed the highest thermal stability with a  $T_{\text{onset}}$  of 298°C, confirming a strong SF contribution.

This improvement in thermal behaviour stems from the  $\beta$ -sheet domains of silk fibroin, which are known for their high thermal stability due to dense intermolecular hydrogen bonds and ordered packing of protein chains [26,27]. Moreover, these  $\beta$ -sheets create thermal diffusion barriers, delaying the onset of degradation by restricting the volatilization of degradation byproducts.

In CNF/SF systems, fibroin not only thermally stabilizes the amorphous cellulose matrix but also promotes char formation, further contributing to the improved thermal profile. These findings align with other protein–polysaccharide composites, where interpenetrating hydrogen-bonded networks reduce chain mobility and enhance resistance to thermal scission [28,29].

From an application perspective, thermal stability up to 298°C makes CS50 suitable for environments involving thermal sterilization, moderate processing temperatures, or thermal load-bearing operations such as food packaging or biomedical implants [30].

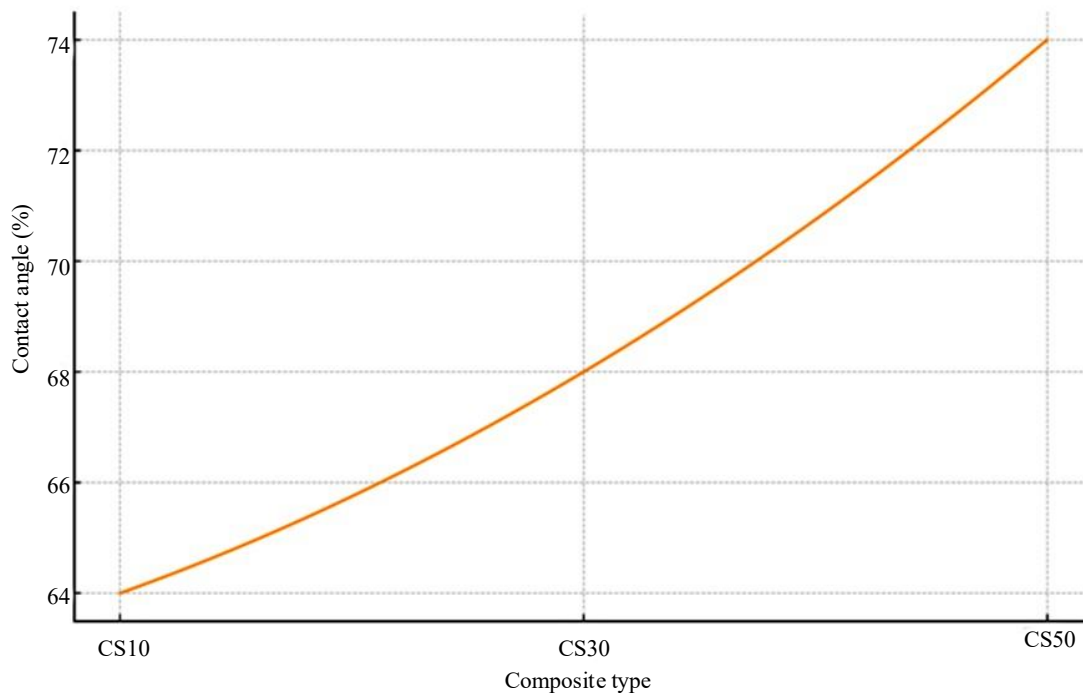


**Figure 5.** Water contact angle of composites.

### Surface Hydrophobicity

Water contact angle (WCA) measurements were conducted to assess the surface wettability of the CNF/SF films, with the outcomes presented in Figure 5. Increasing SF content led to a steady increase in water contact angle:

CS10: 64°

CS30: 68°

CS50: 74°

These results indicate a gradual shift in surface behaviour, becoming less hydrophilic and more water-repellent with increasing SF content. Pure CNFs are inherently hydrophilic due to their abundant hydroxyl groups, which promote water adsorption [31]. However, the addition of SF brings in hydrophobic amino acid residues and  $\beta$ -sheet structures that tend to align at the air–film interface during the casting process, resulting in enhanced water-repelling characteristics of the surface [32].

In addition, the ethanol treatment used to induce  $\beta$ -sheet formation may also drive reorganization of protein chains to the surface, reducing free hydroxyl group availability. This improved hydrophobicity is advantageous in developing moisture-resistant films for applications in packaging and barrier materials [33].

### Water Absorption Behaviour

The ability of the films to absorb water was assessed following a 24-hour immersion period. CS10 absorbed 45% of its dry weight in water, while CS50 absorbed only 28%, indicating a substantial reduction in water uptake as SF content increased.

This behaviour supports the findings from the WCA analysis. Silk fibroin domains create a denser matrix and reduce the accessibility of hydrophilic CNF regions. In essence, internal hydrogen bonding between CNFs and SF lowers the availability of polar functional groups capable of engaging with water molecules [34].

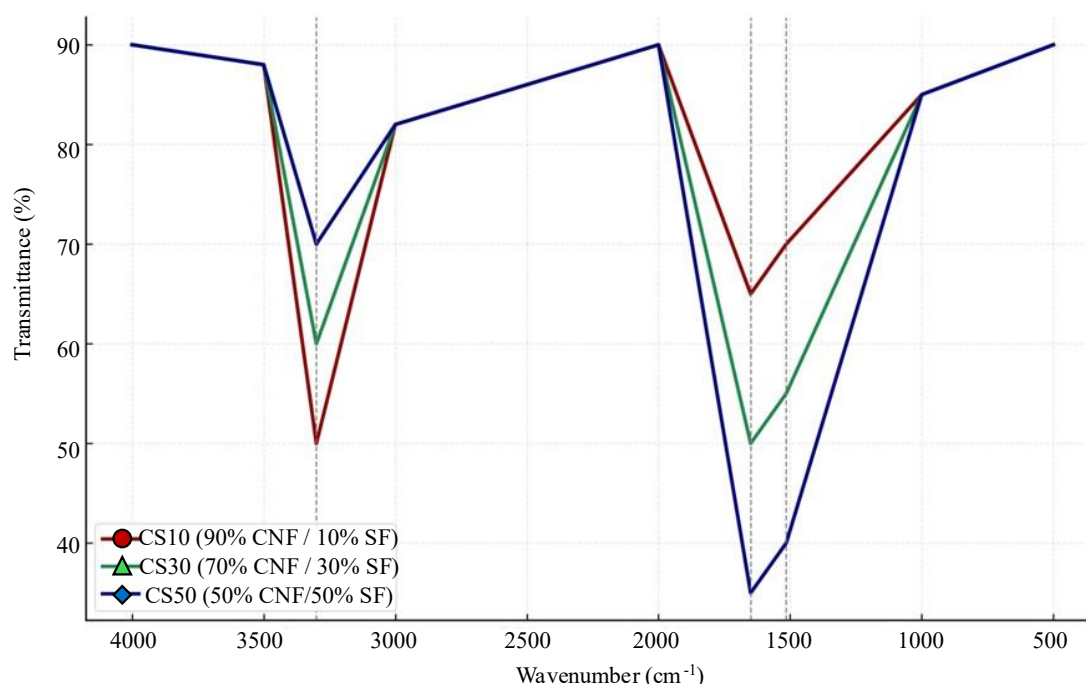


**Figure 6.** FTIR spectra between CNFs and SF with increasing fibroin content.

Moreover, the dense packing induced by  $\beta$ -sheet regions limits the free volume within the matrix, preventing water diffusion. This is highly beneficial in humidity-sensitive applications, where dimensional stability and barrier integrity are critical [35].

### Structural Interactions (FTIR Analysis)

To further confirm the molecular-level interactions between CNFs and SF, FTIR analysis was conducted. All composite films showed characteristic absorption peaks:

Characteristic absorption bands near  $1650\text{ cm}^{-1}$  (Amide I) and  $1515\text{ cm}^{-1}$  (Amide II) correspond to the C=O stretching and N–H bending vibrations, respectively, indicative of the silk fibroin protein backbone. A broad peak around  $3300\text{ cm}^{-1}$ , corresponding to O–H stretching from cellulose.

With increasing SF content, the Amide I and II peaks intensified and shifted slightly, which is a hallmark of increased  $\beta$ -sheet crystallinity in silk fibroin. Simultaneously, the O–H peak from CNFs decreased in intensity, confirming hydrogen bonding between CNF hydroxyls and SF amide groups shown in figure 6 [36,37].

This interaction not only enhances the physical properties of the composite but also suppresses phase separation and leads to better homogeneity. Such structural interplay is vital for tailoring the properties of biopolymer-based films for target-specific performance [38-40].

## CONCLUSION

This study successfully demonstrates the fabrication and characterization of cellulose nanofiber (CNF) and silk fibroin (SF) based biodegradable composite films. By systematically adjusting the SF concentration, valuable insights were obtained into the molecular interactions and how these interactions affect the material's structure, strength, thermal behaviour, and surface water resistance.

The following conclusions were drawn:

- Increasing the silk fibroin (SF) content led to notable improvements in mechanical properties. The tensile strength rose from 72 MPa in CS10 to 112 MPa in CS50, while the Young's modulus doubled from 2.4 GPa to 4.8 GPa, attributed to enhanced stress distribution and the development of  $\beta$ -sheet structures within the SF matrix.

- The composite films exhibited improved resistance to thermal degradation, as evidenced by the rise in onset decomposition temperature from 262 °C (CS10) to 298 °C (CS50), attributed to stronger intermolecular bonding.
- Hydrophobicity and moisture resistance improved, demonstrated by the rise in water contact angle from 64° to 74° and a reduction in water uptake from 45% to 28%, suggesting enhanced dimensional stability under humid conditions.
- FTIR analysis confirmed strong interfacial interactions, with intensified Amide I and II peaks and reduced O–H stretch, validating hydrogen bonding between CNFs and SF molecules.
- The CS50 formulation emerged as the optimal composition, offering the best balance of strength, flexibility, and environmental resilience—suitable for biomedical films, flexible packaging, and sustainable material applications.

## REFERENCES

1. Geyer R, Jambeck JR, Law KL. Production, use, and fate of all plastics ever made. *Sci Adv.* 2017;3(7):e1700782.
2. Andrady AL. Microplastics in the marine environment. *Mar Pollut Bull.* 2011;62(8):1596–1605.
3. Singh B, Sharma N. Mechanistic implications of plastic degradation. *Polym Degrad Stab.* 2008;93(3):561–584.
4. Arrieta MP, Fortunati E, Dominici F, et al. Multifunctional PLA–PHB/cellulose nanocrystal films: Processing, structural and thermal properties. *Carbohydr Polym.* 2014;107:16–24.
5. Klemm D, Heublein B, Fink HP, Bohn A. Cellulose: Fascinating biopolymer and sustainable raw material. *Angew Chem Int Ed Engl.* 2005;44(22):3358–3393.
6. Isogai A, Saito T, Fukuzumi H. TEMPO-oxidized cellulose nanofibers. *Nanoscale.* 2011;3(1):71–85.
7. Moon RJ, Martini A, Nairn J, et al. Cellulose nanomaterials review: structure, properties and nanocomposites. *Chem Soc Rev.* 2011;40(7):3941–3994.
8. Dufresne A. Nanocellulose: From nature to high performance tailored materials. *De Gruyter Open Access.* 2012.
9. Iwamoto S, Nakagaito AN, Yano H. Nano-fibrillation of pulp fibers for the processing of transparent nanocomposites. *Appl Phys A.* 2007;89:461–466.
10. Satyanarayana KG, Arizaga GGN, Wypych F. Biodegradable composites based on lignocellulosic fibers. *Prog Polym Sci.* 2009;34(9):982–1021.
11. Deepa B, Abraham E, Cordeiro N, et al. Utilization of various lignocellulosic biomass for the production of nanocellulose. *Bioresour Technol.* 2011;102(24):11246–11253.
12. Liese W, Köhl M. *Bamboo: The Plant and its Uses.* Springer; 2015.
13. Li Y, Liu Y, Zhou Y, et al. Bamboo cellulose nanofibers and their application in hydrogels: a review. *Cellulose.* 2021;28:1775–1795.
14. Zhang Y, Zhang M, Chen Y, et al. Bamboo-derived CNF/polymer composites: Design, preparation, and performance. *Int J Biol Macromol.* 2020;164:2576–2590.
15. Altman GH, Diaz F, Jakuba C, et al. Silk-based biomaterials. *Biomaterials.* 2003;24(3):401–416.
16. Kundu B, Rajkhowa R, Kundu SC, Wang X. Silk fibroin biomaterials for tissue regenerations. *Adv Drug Deliv Rev.* 2013;65(4):457–470.
17. Rockwood DN, Preda RC, Yücel T, et al. Materials fabrication from Bombyx mori silk fibroin. *Nat Protoc.* 2011;6(10):1612–1631.
18. Meinel L, Hofmann S, Karageorgiou V, et al. Engineering cartilage-like tissue using human mesenchymal stem cells and silk protein scaffolds. *Biotechnol Bioeng.* 2004;88(3):379–391.
19. Vepari C, Kaplan DL. Silk as a biomaterial. *Prog Polym Sci.* 2007;32(8–9):991–1007.
20. Huang J, Wang X, Zhan X, et al. Synergistic strengthening of silk fibroin composites by cellulose nanofibers: morphology, mechanics and structure–property relationships. *Carbohydr Polym.* 2019;225:115236.
21. Liu Y, Du H, Zeng J, et al. Recent advances in cellulose-based composite materials for sustainable packaging. *Carbohydr Polym.* 2021;261:117888.

22. Tanpichai S, Quero F, Nogi M, Yano H. Transparent cellulose nanofiber reinforced silk fibroin biocomposite films. *Biomacromolecules*. 2019;20(4):1531–1538.
23. Kim UJ, Park J, Kim HJ, Wada M, Kaplan DL. Three-dimensional aqueous-derived biomaterial scaffolds from silk fibroin. *Biomaterials*. 2005;26(15):2775–2785.
24. Wang X, Yan C, Wang H, et al. Flexible cellulose-silk fibroin nanocomposite films for food packaging. *J Mater Chem B*. 2022;10(9):1798–1807.
25. Mahat M, Behera D, Nayak SK. Thermal analysis and degradation behavior of SF-CNF composites. *J Therm Anal Calorim*. 2020;139(6):3849–3859.
26. Li J, Ren T, Song D. Thermal degradation behavior of CNF-reinforced biopolymers. *Polym Degrad Stab*. 2019;166:248–256.
27. Lin N, Dufresne A. Nanocellulose in biocomposites: recent advances. *Eur Polym J*. 2014;59:302–325.
28. Costa SM, Ferreira DP, Alves R, et al. Eco-friendly silk fibroin/cellulose nanofiber films: Physicochemical and barrier performance. *Ind Crops Prod*. 2022;177:114481.
29. Siqueira G, Bras J, Dufresne A. Cellulosic bionanocomposites: a review of preparation, properties and applications. *Polymers*. 2010;2(4):728–765.
30. Ren H, Sun Q, Li Y, et al. Hydrophobic cellulose-based bioplastics reinforced with natural proteins. *Carbohydr Polym*. 2020;247:116687.
31. Choudhary R, Kumar A. Cellulose nanofiber-reinforced silk fibroin biofilms with enhanced barrier and hydrophobic properties. *Cellulose*. 2021;28(8):4795–4811.
32. Paul U, Jain D, Ray SS. Biodegradable CNF/SF composites with enhanced moisture resistance. *Green Mater*. 2022;10(2):78–88.
33. Reddy K, Reddy M, Jiang Q. Bio-inspired CNF/silk fibroin composites for high humidity resistance. *ACS Appl Mater Interfaces*. 2020;12(41):46658–46668.
34. Ramakrishnan SK, Palanisamy S, Khan T, Ajithram A, Ahmed OS. Mechanical, morphological and wear resistance of natural fiber/glass fiber-based polymer composites. *BioResources*. 2024;19(2):3271–3289. doi:10.15376/biores.19.2.3271-3289
35. Palanisamy S, Kalimuthu M, Palaniappan M, Alavudeen A, Rajini N, Santulli C. Characterization of *Acacia caesia* bark fibers (ACBFs). *J Nat Fibers*. 2021;18(15):10241–10252. doi:10.1080/15440478.2021.1993493
36. Murugesan P, Palaniappan M, Santulli C, et al. Physico-chemical characterization of *Grewia Monticola* Sond (GMS) fibers for prospective application in biocomposites. *J Nat Fibers*. 2022;19(17):15276–15290. doi:10.1080/15440478.2022.2123076
37. Palaniappan M, Palanisamy S, Murugesan TM, et al. Novel *Ficus retusa* L. aerial root fiber: a sustainable alternative for synthetic fibres in polymer composites reinforcement. *Biomass Convers Biorefinery*. 2025;15(5):7585–7601. doi:10.1007/s13399-024-05495-4
38. Palanisamy S, Kalimuthu M, Palaniappan M, Santulli C, Nagarajan R, Fragassa C. Tailoring epoxy composites with *Acacia caesia* bark fibers: evaluating the effects of fiber amount and length on material characteristics. *Fibers (Basel)*. 2023;11(7):63. doi:10.3390/fib11070063
39. Sumesh KR, Palanisamy S, Khan T, Ajithram A, Ahmed OS. Mechanical and wear performance evaluation of natural fiber/epoxy matrix composites. *BioResources*. 2024;19(4):8459–8478. doi:10.15376/biores.19.4.8459-8478
40. Palanisamy S, Kalimuthu M, Azeez A, Palaniappan M, Dharmalingam S, Nagarajan R, Santulli C. Wear properties and post-moisture absorption mechanical behavior of Kenaf/Banana-fiber-reinforced epoxy composites. *Fibers (Basel)*. 2022;10(4):32. doi:10.3390/fib10040032